# Marine and Terrestrial Organic Ice Nucleating Particles in Pristine Marine to Continentally-Influenced Northeast Atlantic Air Masses

**Christina S. McCluskey[1,2], Jurgita Ovadnevaite[3], Matteo Rinaldi[4], James Atkinson[5], Franco Belosi[4], Darius Ceburnis[3], Salvatore Marullo[6,7], Thomas C. J. Hill[1], Ulrike Lohmann[5], Zamin A. Kanji[5], Colin O'Dowd[3], Sonia M. Kreidenweis[1], Paul J. DeMott[1]**

[1]Department of Atmospheric Science, Colorado State University, Fort Collins, CO, USA.

[2]Now at Advanced Study Program, National Center for Atmospheric Research, Boulder, CO, USA

[3]School of Physics, National University of Ireland Galway, Galway, Ireland

[4]Institute of Atmospheric Sciences and Climate, CNR, Bologna, Italy.

[5]Institute of Atmospheric and Climate Science, ETH Zurich, Switzerland

[6]ENEA, Centro Ricerche Frascati, Italy

[7]Institute of Atmospheric Sciences and Climate, CNR, Roma, Italy.

Corresponding author: Christina McCluskey (mccluscs@atmos.colostate.edu)

**Key Points:**

- Pristine sea spray aerosol is a dominant regional source of ice nucleating particles at a remote North Atlantic coastal site
- Ice nucleating particles at a remote North Atlantic coastal site were largely comprised of organic carbon and/or heat labile material
- Sea spray aerosol is associated with a factor of 1000 fewer ice nucleating sites per surface area of aerosol compared to mineral dust.



This article has been accepted for publication and undergone full peer review but has not been through the copyediting, typesetting, pagination and proofreading process which may lead to differences between this version and the Version of Record. Please cite this article as doi: 10.1029/2017JD028033

**Abstract**

Sea spray aerosol (SSA) generated by bubble bursting at the ocean surface is an important component of aerosol-cloud interactions over remote oceans, providing the atmosphere with ice nucleating particles (INPs), or particles required for heterogeneous ice nucleation. Studies have shown that organic INPs are emitted during phytoplankton blooms, but changes in INP number concentrations ($n_{INPs}$) due to ocean biological activity have not been directly demonstrated in natural SSA. In this study, a clean sector sampler was used to differentiate ice nucleation and composition of pristine SSA from terrestrial aerosol at the Mace Head Research Station (MHD) in August 2015. Average $n_{INPs}$ active at -15 °C ($n_{INPs,-15\ °C}$) were 0.0011 $L^{-1}$ and large variability (up to a factor of 200) was observed for INPs active warmer than -22 °C. Highest $n_{INPs}$ in the clean sector occurred during a period of elevated marine organic aerosol from offshore biological activity (M1, $n_{INPs,-15\ °C}$ = 0.0077 $L^{-1}$). A peak in $n_{INPs}$ was also observed in terrestrial organic aerosol (T1, $n_{INPs,-15\ °C}$ = 0.0076 $L^{-1}$). The impacts of heating and hydrogen peroxide digestion on $n_{INPs}$ indicate that INPs at MHD were largely organic and that INPs observed during M1 and T1 were biological (i.e., protein-containing). Complexities of predicting increases in $n_{INPs}$ due to offshore biological activity are explored. A parameterization for pristine SSA INPs over the North Atlantic Ocean was developed, illustrating that SSA is associated with a factor of 1000 fewer ice nucleating sites per surface area of aerosol compared to mineral dust.

## 1 Introduction

Ice phase transitions in mixed phase clouds are poorly represented in numerical models (McCoy et al., 2015, McCoy et al., 2016), leading to uncertainties in simulated cloud phase (liquid/ice) partitioning, precipitation rates and atmospheric radiative transfer. Notably, numerical models struggle to match observed cloud phase partitioning in high latitude clouds, leading to significant modeled energy biases that impact simulated climate sensitivity estimates (Tan et al., 2016). Atmospheric ice nucleating particles (INPs), by enabling heterogeneous ice formation, play an important role within these complex aerosol-cloud-climate interactions. Over remote oceans, terrestrial sources of immersion freezing INPs (e.g., mineral dust) are often absent and sea spray aerosol (SSA), resulting from wave breaking and bubble bursting at the ocean surface, may serve as the primary source of INPs (Burrows et al., 2013; Vergara-Temprado et al., 2017). While some studies have investigated ice nucleation of SSA in cirrus conditions (e.g., Schill and Tolbert, 2014; Ladino et al., 2016), this study focuses on immersion ice nucleation of SSA in the mixed phase regime.

The chemical complexity of aerosol production at the ocean surface needs to be considered in investigations of marine INPs. Previous studies have revealed the low ice nucleating ability of SSA relative to terrestrial sources in the immersion freezing mode (DeMott et al., 2016), and the high amounts of supercooled liquid in remote marine regions (Huang et al., 2015) suggest that cloud glaciation may be inhibited by this lack of INPs. However, using an extensive survey conducted by Bigg (1973), Schnell and Vali (1976) demonstrated that higher INP emissions were collocated with ocean regions that were expected to be biologically productive (i.e., phytoplankton blooms). They also observed higher INP number concentrations per volume of phytoplankton-rich seawater compared to seawater with little phytoplankton biomass, proposing a possible biogenic source of INPs from ocean waters. If true, modeling studies have found that this link may have fundamental implications for ice phase transition over remote oceans (Burrows et al., 2013; Vergara-Temprado et al., 2017). Elucidating this biologically-mediated mechanism for enhanced oceanic INP emissions is needed to accurately estimate atmospheric INP number

concentrations and consequent primary ice formation in clouds over high latitude remote regions.

SSA composition comprises of a mixture of seawater (SW) and sea surface microlayer (SML, the upper 50 to 250 μm of the ocean surface; Zhang et al., 1998, van Pinxteren et al., 2017) components, including sea salts and organic matter (e.g., Gantt et al., 2013). Total organic carbon (TOC) in these components includes particulate organic carbon (POC, e.g., phytoplankton, bacteria) and dissolved organic carbon (DOC, e.g., organic molecules and exudates). The SML can be significantly enriched with both POC and DOC relative to the bulk SW, which can then transfer to the aerosol phase (e.g., van Pinxteren et al., 2017). Many variables control the transfer of organic species from the ocean surface to the aerosol; known parameters include the species solubility (Cochran et al., 2016; van Pinxteren et al., 2017), biological productivity and wind speed (Gantt et al., 2011; Rinaldi et al., 2013). However, recent studies suggest that additional variables, such as bacterial abundance or sea surface temperature, should also be considered (van Pinxteren et al., 2017).

Wilson et al. (2015) found a positive relationship between TOC mass concentrations and number concentrations of ice nucleating entities (INEs) in SML samples collected in the North Atlantic Ocean. During mesocosm laboratory studies of nascent SSA throughout the course of two separate phytoplankton blooms, McCluskey et al., (2017) found increases in number concentrations of INPs active at a range of temperatures in SSA associated with changes in biological activity. Furthermore, McCluskey et al., (2018) reported evidence for both marine microbes (i.e., POC) and macromolecules (i.e., DOC) as important contributors to INP populations found in nascent sea spray from laboratory mesocosm studies. While these studies support the link proposed by Schnell and Vali (1976), increased marine INP number concentrations in marine organic aerosol emissions from biologically productive ocean waters has not been explored in ambient aerosol.

There are many challenges for observing this phenomenon in the ambient atmosphere. As mentioned previously, terrestrial aerosols are more ice nucleation active than SSA (e.g., DeMott et al., 2016), making it difficult to distinguish marine organic from terrestrial aerosol influences. Additionally, remote INP number concentrations are low (< 0.02 $L^{-1}$ at -15 °C, DeMott et al., 2016), thus requiring a measurement approach that allows large sampling volumes and has low INP detection limits. In this study, we monitor INP number concentrations at the Mace Head Research Station (MHD), located on the west coast of Ireland, which has been utilized as a natural laboratory for pristine marine aerosol research for over 50 years. Our goal was to characterize INPs in pristine marine air and to investigated the influence of marine organic aerosol plumes associated with offshore biological activity (O'Dowd et al., 2004, Ovadnevaite et al., 2011) on INP populations at MHD.

## 2 Methods

### 2.1 Study Overview

Various measurements were made as part of an INP detection intercomparison project at the MHD (53.32 °N, 9.90 °W, Figure S1) from 5-29 August 2015. Measurements were made approximately 100 m inland from the coastline. Immersion freezing INP number concentrations ($n_{INPs}$) were measured using offline and online techniques: the offline Ice Spectrometer (IS, Colorado State University), online Horizontal Ice Nucleation Chamber – Evaporation (HINC-EV, ETH Zurich), and offline Dynamic Filter Processing Chamber (DFPC, National Research Council, Italy). An aerodynamic particle sizer, scanning electrical mobility particle sizer, tapered element oscillating microbalance, and aerosol mass spectrometer were used to characterize aerosol size distributions, mass, and composition (as

detailed below). Meteorological conditions were also monitored, including wind speed and direction. All dates and times reported here are local unless otherwise stated.

## 2.2 Ice nucleation measurements

### 2.2.1 Ice spectrometer

The ice spectrometer is an offline measurement technique used to determine number concentrations of immersion freezing INPs in aerosol samples. Following the methods of McCluskey et al., (2017), Nuclepore™ track-etched polycarbonate membrane filters (47 mm diameter, Whatman, GE Healthcare Life Sciences) with pore size of 0.05 μm were pre-cleaned with 10% $H_2O_2$ and rinsed with filtered deionized water (18 megaohms (mΩ) deionized water that was passed through a 0.02-μm pore Anotop syringe filter (Whatman)). Filters were cleaned and dried on aluminum foil, in a laminar flow cabinet under high-efficiency filtered air flow (< 0.01 particles ($D_p$ > 4 nm) $cm^{-3}$). Nalgene analytical filter units (Nalgene Nunc Int.) were pre-packed with the pre-cleaned filters, which were overlaid on top of the existing 0.45 μm filter, placed in Ziplock® bags and shipped to MHD for use.

During this study, two filters for IS processing were collected daily at the top of the 10-meter mast: a CLEAN sector and an ALL filter. Total sample collection periods ranged from 6 - 37 hrs (20 hrs on average) and, on average, 6555 L and 6024 L of air was collected on the CLEAN and ALL sector filters, respectively. The pump for the CLEAN sector filter was powered using the MHD Clean Sector Sampler (Rinaldi et al., 2009). This sampler supplies power to the sampling pump only when equivalent black carbon (eBC), measured by a Thermo scientific multi-angle absorption photometer (MAAP) instrument (Thermo Fisher Scientific Inc., Waltham, MA, model 5012), is less than 15 ng/$m^3$ and wind direction is between 190 to 300 degrees (Figure S1). The pump for the ALL filter was powered continuously during the total collection period. CLEAN sector filters represent aerosol from pristine marine air and ALL filters represent aerosol from all sources. With the filter specifications and flow rates used in this study, following collection efficiency tables provided by Spurny and Lodge (1972) and also used by DeMott et al. (2016), we estimate 99% or more of the total suspended particles ($D_p$ > 0.05 μm) were collected by the open-face filter holders. After collection, filters were removed from filter holders with sterile tweezers and stored in sterile petri dishes sealed with Parafilm. Frozen filters (-20 °C) were shipped to CSU and remained frozen until IS analysis (Methods S2). Some filters were contaminated with rain or fog water; these samples were not used in this analysis.

Particles were recovered by suspending filters in room-temperature 7 mL of filtered deionized water (following same method for filter cleaning) and shaken for 20 minutes using an end-over-end shaker (Rototorque, Cole-Palmer). The sample suspension was then dispensed (50 μL aliquots) into 24 or 32 wells of a PCR tray (96-well plate, μCycler) that was then inserted into the IS aluminum blocks (Hiranuma et al., 2015). Coolant is circulated through copper pipes embedded within heat exchange plates that encase the sides and base of the IS, cooling the IS over its effective range, from 0 °C to -27 °C, at 0.33 °C $min^{-1}$. Using methods developed by Vali (1971), counts of frozen wells at 0.5 – 1 °C intervals were used to determine $n_{INPs}$ as a function of temperature. Binomial sampling confidence intervals (95%, formula 2, Agresti and Coull, 1998) were used to describe counting statistic uncertainties, and seven blank filters were analyzed to account for method contamination (i.e., INPs introduced during preparation and analysis).

Additional IS trials were performed to explore properties of the collected INPs. McCluskey et al. (2018) proposed two classes of marine INPs. Ice nucleating particulate

organic carbon (IN-POC) comprises IN-active microbes or microbial fragments, which are heat-labile. Ice nucleating dissolved organic carbon (IN-DOC) is described as IN-molecules that are not heat-labile. The contributions of these two marine INP classes were investigated by performing offline treatments described by McCluskey et al. (2018). To determine the contribution of heat-labile material to the collected INP populations, sample suspensions were heated to 95 °C for 20 minutes, cooled to room temperature and then analyzed in the IS. Aliquots from aerosol filter suspensions were also digested with hydrogen peroxide to decompose all organic INPs. 1 mL of the suspension was combined with 0.5 mL of 30% $H_2O_2$ (Sigma Aldrich) to achieve a final concentration of 10%, then the mixture was immersed in water, heated to 95 °C for 20 min while being illuminated with two, 26 W UVB fluorescent bulbs. To remove residual $H_2O_2$ (to prevent otherwise significant freezing point depression), catalase (Cat. number 100429, MP Biomedicals) was added to the cooled solution. The enzyme was added in several 20 µL aliquots, allowing several minutes between each, until no effervescence resulted upon its addition. At each temperature, Fisher's Exact Test (*Fisher*, 1922) was used to determine *p* values to describe the significance of measured changes in the proportion of wells frozen after treatments. At each temperature, the *p* value is estimated from the total number of wells being tested in both samples (*n*), the number of wells frozen and unfrozen in the untreated sample (*a* and *b*, respectively) and in the treated sample (*c* and *d*, respectively):

$$p = \frac{(a+b)!\,(c+d)!\,(a+c)!\,(b+d)!}{a!\,b!\,c!\,d!\,n!}$$

In this study, values are considered statistically different if they have a *p* value of less than 0.05.

2.2.2. Horizontal Ice Nucleation Chamber – Evaporation

Constructed and operated by ETH Zürich, the HINC-EV is a horizontal Continuous Flow Diffusion Chamber (CFDC) closely resembling the University of Toronto CFDC (UT-CFDC, Kanji and Abbatt, 2009) and almost identical to the HINC previously built at ETH Zurich (Lacher et al., 2017). The principle difference between HINC and HINC-EV is the conversion of a portion of the chamber into an evaporation section. For more details on the horizontal CFDC concept and UT-CFDC/HINC design please see Kanji and Abbatt (2009) and Lacher et al. (2017), respectively.

The HINC-EV consists of two horizontal parallel copper plates, an upper wall and a lower wall, which are temperature controlled by an external chiller. Humidity inside the chamber is provided by wet glass fiber filter papers on each wall, which are frozen into ice layers as the chamber is cooled. Supersaturation with respect to water ($S_w$) at the centerline of the chamber (a horizontal plane equidistant from the two chamber walls) is realized by inducing a temperature difference between the two chamber walls. The first section serves as a nucleation and growth section where ice will grow rapidly. The last 8.7 cm (equivalent to an aerosol residence time of 2.7 s) of HINC-EV is an evaporation section, kept at approximately ice saturation ($S_i = 1$) by maintaining the upper and lower walls at the same temperature.

Dried aerosol is introduced, and preconditioned to the centerline temperature, via an injector pipe at a distance of 18.7 cm from the HINC-EV outlet (corresponding to a growth section aerosol residence time of 5.7 s). The aerosol stream is surrounded by a sheath flow of particle-free pure nitrogen (zero grade - 99.998 % $N_2$), which is preconditioned to the chamber temperature and $S_w$ prior to encountering the aerosol stream at the chamber head. The ratio of sheath air to sample air was 8:1. On leaving the injector, the aerosol stream is

exposed to the centerline $S_w$ and can act as either an INP (in the deposition and/or condensation mode depending on the centerline $S_w$) or a cloud condensation nuclei (CCN) and consequently as a possible immersion mode INP. In the evaporation section, activated CCN that are absent of immersion mode INPs evaporate, leaving an aerosol distribution containing dry particles and large ice particles. At the exit of the chamber, an optical particle counter measures the aerosol and ice particles; ice particles are counted by assuming that any nucleated INPs have grown to diameters greater than 4 µm. During operation of HINC-EV, INPs are counted over 15 second intervals. If no INPs are observed in the 15 second counting interval, the reported number of INPs is zero for that sampling interval. Data collected every 15 seconds, including zeros, are reported here as averages over approximately 20 min periods. Filtered (particle-free) air is sampled for 10 min between each 20 min sample to quantify the amount of erroneous ice from the chamber rather than from aerosol (i.e., background counts). Ambient measurements that are less than one standard deviation of the background concentration are classified as below the limit of detection and thus assumed to be an unreliable representation of an ambient INP concentration (Lacher et al., 2017).

During this study, ambient particles were sampled isokinetically from a sampling inlet located at the same height as the 10 m mast, which included 12 meters of 2.54 cm diameter stainless steel tubing with a total sample flow of 12.5 Lpm. Before entering HINC-EV, aerosol passed through approximately 1 m of 1.9 cm conductive tubing and 3 m of horizontally oriented diffusion driers to remove the abundant ambient moisture that can result in a rapid increase in instrument background counts. The residence time of particles in the sampling inlet was approximately 25 seconds. Before injection into HINC-EV, total aerosol concentration was measured using a condensation particle counter. Due to gravitational settling in the driers, the maximum particle size cut-off samples by HINC-EV has an estimated $D_{50}$ of 2 µm (Lacher et al., 2017) and thus this measurement includes all particles less than 2 µm. Finally, measurements at MHD were conducted at 243 K and $S_w$ of 1.04, corresponding to $S_i$ of 1.4. Uncertainties in chamber sampling conditions are estimated to be ± 0.4 K, $S_w$ ± 0.02 and $S_i$ ± 0.03.

2.2.3 Dynamic Filter Processing Chamber

The Dynamic Filter Processing Chamber (DFPC) is a replica of the diffusion chamber described by Langer and Rogers (1975). Atmospheric $n_{INPs}$ active at -22 °C are detected via offline processing of membrane filters, following the procedure described in Santachiara et al. (2010) and Belosi et al., (2017). Briefly, $PM_1$ and $PM_{10}$ aerosol fractions were simultaneously sampled on nitrocellulose membrane filters (Millipore HABG04700, nominal porosity 0.45 µm) by mounting different sampling heads (1 µm, and 10 µm cut-point-Standard EN 12341, TCR Tecora) in front of the filters. Sampling was carried out on the 10 meter mast (same as IS filters) only in the CLEAN sector. Samples were returned to the Italian National Research Council (ambient temperature) for analysis, where collected filters were placed onto a metal plate, previously covered with a smooth surface of Vaseline. Subsequently, the Vaseline was slightly heated (70 °C for 10 s) and rapidly cooled in order to fill the filter pores and create effective thermal contact. The metal plate was inserted into the DFPC, housed in a refrigerator, to detect and determine the concentration of aerosol particles active as INPs at -22 °C and supersaturation with respect to water of 1.02 (condensation freezing mode). It is assumed that these conditions represent immersion freezing, following the discussion of Vali et al. (2015) that condensation freezing and immersion freezing are not distinguishable as distinct. Five blanks (unsampled filters) were analyzed to account for contaminations during the INP quantification procedure and the results were corrected accordingly.

2.3 Aerosol size and Chemistry

Aerosol size distribution instrumentation was housed in the MHD laboratory, measuring ambient aerosol from a 100 mm diameter stainless steel laminar flow community inlet (Kleefeld et al., 2002). This inlet is located 10 meters above ground level, limiting local influences of aerosol produced along the coastline. Smaller particles ($0.02\ \mu m < D_p < 0.5\ \mu m$) were monitored using a scanning mobility particle sizer (SMPS), where aerosols are neutralized (Kr-85, TSI Model 3077), size-selected based on their mobility diameter (differential mobility analyzer, TSI Model 3071) and counted (condensation particle counter, TSI Model 3010). An aerodynamic particle sizer (APS, TSI Model 3321) was used to measure supermicron ($0.5 < D_p < 20\ \mu m$) size distributions. Aerosol sizing instruments were located downstream of Naphion driers (RH < 40%) and thus size distributions refer to aerosol dry diameter. Sanchez et al. (2017) reported aerosol size distribution data used in this study.

Aerosol mass concentrations were monitored with a tempered element oscillating microbalance (TEOM, Thermo Scientific, Model 1405-DF), which measures fine ($PM_{2.5}$) and coarse ($PM_{2.5-10}$) particle mass fractions simultaneously. A virtual impactor is used to split the $PM_{2.5}$ from $PM_{2.5-10}$ and flow is dried below 20% RH by Nafion driers before arriving on the oscillating microbalances, which were kept at 30 °C. While low temperatures should have prevented volatilization of collected aerosol, slightly negative concentrations still occurred. Negative concentrations were observed after changes in air mass and particulate loading, particularly during rapid shifts from high aerosol loadings (polluted or high SSA) to low aerosol loadings (pristine air masses). The measurements were made at 6 min intervals and this time interval was sometimes insufficient to reach equilibrium, resulting in a mass drop and negative concentration. Leak checks have been routinely performed according to operational procedures. Detection limit and measurement precision was in the order of 1-2 $\mu g/m^3$ and the resolution was better than 1 $\mu g/m^3$ as per instrument specification (Thermo Fisher Scientific).

Aerosol composition was measured with an Aerodyne Research Inc. high resolution time-of-flight aerosol mass spectrometer (HR-ToF-AMS) which provides real-time size resolved composition of volatile and semi-volatile particulate matter (DeCarlo et al., 2006). The HR-ToF-AMS quantifies non-refractory aerosol chemical composition, covering major inorganic species such as ammonium ($NH_4$), sulfate ($SO_4$), nitrate ($NO_3$), and organic species (Org) (Jimenez et al., 2003) in the submicron size range (approximately $PM_1$) (Canagaratna et al., 2007). Quantitative sea salt (SS) concentrations can also be derived following the method described by Ovadnevaite et al., 2012. MSA was measured according to the method described in Ovadnevaite et al. (2014), where the total concentration was derived by scaling the $CH_3SO_2^+$ and $CH_3SO_3H^+$ ions representative of MSA only. A nafion drier was installed in front of the HR-ToF-AMS sampling inlet to reduce relative humidity of the sample to <40%. The HR-ToF-AMS measurements were performed at a time resolution of 5 min and a vaporizer temperature of ~650 °C. The instrument was routinely calibrated (3 times per 1 month) according to the methods described in Jimenez et al. (2003) and Allan et al. (2003). The composition-dependent collection efficiencies (Middlebrook et al., 2012) for the measurement periods discussed in this study ranged from 0.45 to 0.93 for all species, except sea salt. Collection efficiency (CE) of 1 was applied for the sea salt as the effects of both relative ionization efficiency (RIE) and CE were already included into the calibration factor. ToF-AMS HR Analysis 1.12G version was used for the high resolution data analysis.

The origins of air masses were determined for focus periods based on back trajectories (72 hr, 500 m AGL) that were simulated using the National Oceanic and Atmospheric Administration (NOAA) HY-SPLIT model (Stein et al., 2015,

http://www.arl.noaa.gov/HYSPLIT_info.php). A detailed distribution of the back trajectory analyses is provided in Methods S1. Ocean surface Chl *a* concentrations, an indicator for ocean phytoplankton biomass, were sourced from the NASA AQUA/MODIS product for August 2015.

2.4 Satellite derived Chlorophyll a concentrations

Daily Chlorophyll *a* concentrations were downloaded from CMEMS (Copernicus Marine Environment Monitoring Service) and remapped at 25 by 25 km. Missing data due to cloud coverage were reconstructed using the Multichannel Singular Spectrum Analysis (MSSA) algorithm (Ghil et al., 2002), following the same approach as Rinaldi et al. (2013).

## 4 Results and Discussions

4.1 Overview of organic aerosol events during the campaign

Number concentrations of INPs active at -15 °C ($n_{INPs,-15\ °C}$, measured by the IS), submicron organic aerosol mass concentrations ($M_{Org}$), equivalent black carbon mass concentrations ($M_{eBC}$) and meteorology (wind direction and speed) timelines are shown in Figure 1. Additional submicron aerosol chemistry (Figure S2), particulate matter mass concentrations ($PM_{2.5}$ and $PM_{10}$) and meteorological data are summarized in Table 1 and Figure 2. The study average $M_{Org}$ measured in ALL sectors was 0.33 (±0.38) μg $m^{-3}$ and included three periods of elevated $M_{Org}$ that were studied to investigate the influence of organic aerosol plumes on INP populations at MHD.

Two periods of elevated organic aerosol were classified as marine organic events: the first marine organic event (M1) was sampled by the IS from 9 Aug 11:43 to 9 Aug 19:10 and the second marine organic event (M2) was sampled by the IS from 12 Aug 19:52 to 14 Aug 09:47 (Figure 1). Air sampled during M2 arrived from the marine sector (CLEAN sector wind direction is 190 to 300°, Figure 1e), but $M_{eBC}$ (18 ±11 ng $m^{-3}$,Table 1) were slightly above the CLEAN sector threshold (15 ng $m^{-3}$). HYSPLIT back trajectories and ocean surface Chl *a* concentrations (Figure 3) show that the sampled air masses passed over biologically active ocean regions during M1 and M2, where air masses associated with M2 passed over oceanic regions further north compared to M1. During M1 and M2, terrestrial chemical markers, including ammonium ($NH_4$), nitrate ($NO_3$) and *eBC*, were lower or similar to the study average (Table 1, Figure 2). $M_{Org}$ was 0.85 (±0.20) μg $m^{-3}$ during M1, approximately a 4-fold increase from neighboring periods, and $M_{Org}$ was 0.57 (±0.25) μg $m^{-3}$ during M2. Submicron sea salt aerosol mass concentrations during M2 (0.12 ±0.13 μg $m^{-3}$) and M1 (0.15 ±0.06 μg $m^{-3}$) were similar to the whole study average (0.15 ±0.16 μg $m^{-3}$). Assuming marine emissions were the only source of organic aerosol during M1 and M2, the lower $M_{Org}$ during M2 compared to $M_{Org}$ during M1 suggests that aerosol observed during M1 may have been more enriched with organic matter compared to M2. However, the single particle organic enrichment or mixing state was not measured during this study. While HR-ToF-AMS mass spectra for submicron organic particles observed during M1 (Figure S4) and M2 (Figure S5) were similar to those previously observed in association with offshore biological activity (Ovadnevaite et al., 2011), mass spectra during M2 (Figure S5) contained a higher signal from methanesulfonic acid (MSA, m/z 79) compared to M1, possibly due to slightly higher contributions from marine secondary organic aerosol (Rinaldi et al., 2010). This is also evident in the mass contribution of MSA to total aerosol mass measured by the HR-ToF-AMS (Figure S3).

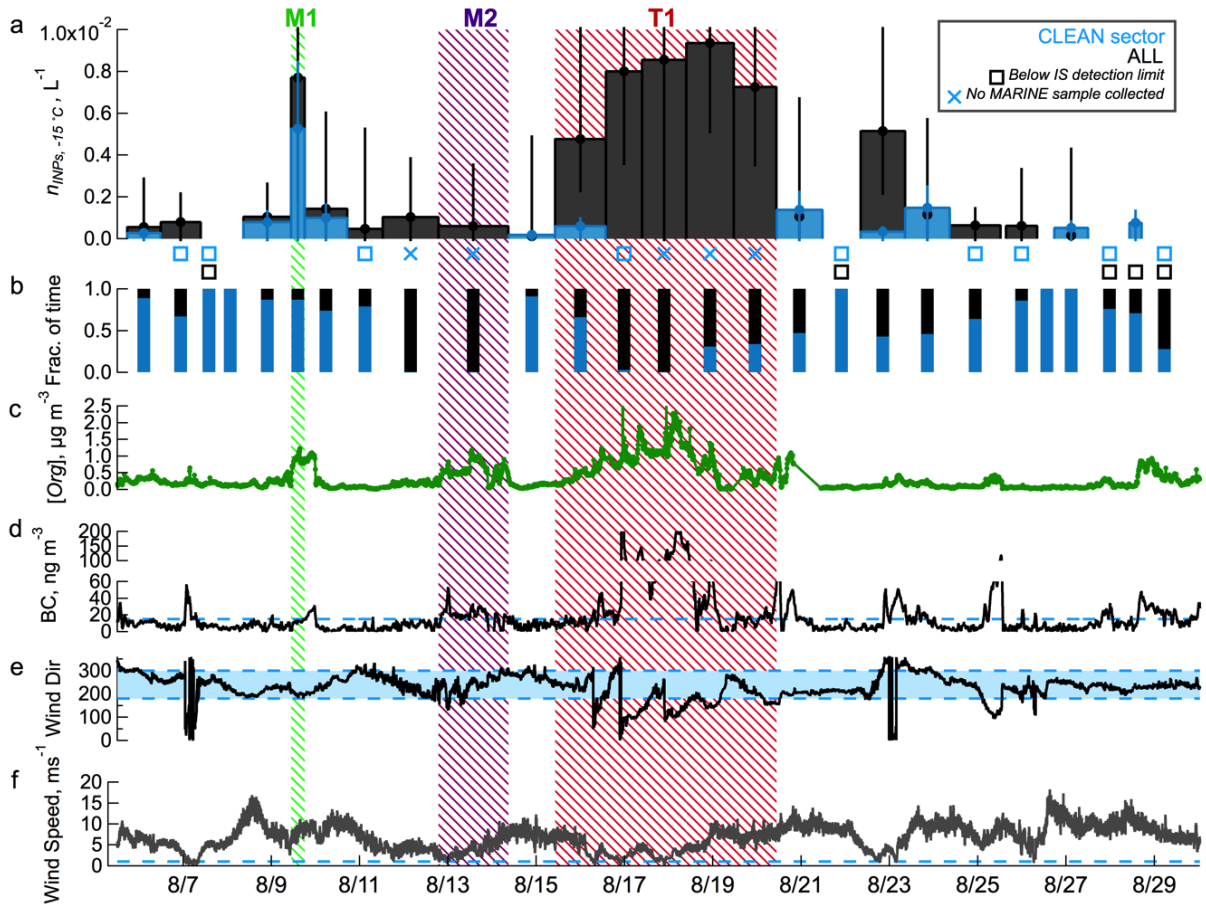


**Figure 1**. **a**) Timeline of INP number concentrations active at -15 °C ($n_{INPs,-15°C}$) for ALL (black) and CLEAN sector (blue) samples. Open square markers indicate measured $n_{INPs,-15°C}$ that were below detection limit. Cross markers indicate that a sample was not collected for that sampling period. Vertical bars are the 95% confidence intervals for IS measurements. **b**) Fraction of sampling time that was in the CLEAN sector (blue) versus non-clean sectors (black). Timeline of **c**) organic carbon mass concentrations measured by the HF-ToF-AMS, **d**) equivalent black carbon (eBC) mass concentrations, **e**) wind direction (Wind Dir), and f) wind speed. Green, purple and red shadings correspond to organic events M1, M2, and T1. In d-e, thresholds used to define CLEAN sector periods are shown in light blue for eBC, wind direction and wind speed.

**Table 1.** Summary of number concentrations of INPs active at -15 °C ($n_{INPs}$), aerosol chemistry, particulate matter (PM) and meteorology, showing averages and standard deviations for the entire study and for the selected periods M1, M2 and T1. Submicron aerosol composition includes ammonium ($NH_4$), nitrate ($NO_3$), sulfate ($SO_4$), organic matter (Org), sea salt (SS), methanesulfonic acid (MSA), and total equivalent black carbon (eBC).

| | **Study** | **M1** | **M2** | **T1** |
|---|---|---|---|---|
| *Ice nucleating particle number concentration (T = -15 °C)* | | | | |
| ALL $n_{INPs}$ ($L^{-1}$) | 0.0030 ± 0.0033 | 0.0077* | 0.0006** | 0.0076 ±0.0018 |
| CLEAN $n_{INPs}$($L^{-1}$) | 0.0011 ±0.0014 | 0.0053*** | no sample | 0.0006**** |
| *Aerosol composition* | | | | |
| $M_{NH4}$ (µg $m^{-3}$) | 0.06 ±0.09 | 0.07 ±0.02 | 0.04 ±0.02 | 0.15 ±0.15 |

| | | | | |
|---|---|---|---|---|
| $M_{NO3}$ (μg m$^{-3}$) | 0.03 ±0.04 | 0.02 ± 0.005 | 0.02 ±0.01 | 0.07 ±0.08 |
| $M_{SO4}$ (μg m$^{-3}$) | 0.39 ±0.31 | 0.51 ±0.18 | 0.47 ±0.22 | 0.62 ±0.49 |
| $M_{Org}$ (μg m$^{-3}$) | 0.33 ±0.38 | 0.85 ±0.20 | 0.57 ±0.25 | 0.75 ±0.53 |
| $M_{SS}$ (μg m$^{-3}$) | 0.15 ±0.16 | 0.15 ±0.06 | 0.12 ±0.13 | 0.07 ±0.07 |
| $M_{MSA}$ (μg m$^{-3}$) | 0.03 ±0.02 | 0.03 ±0.01 | 0.04 ±0.02 | 0.04 ±0.02 |
| $M_{eBC}$ (ng m$^{-3}$) | 21 ±53 | 10 ±5 | 18 ±11 | 57 ±106 |
| *Aerosol Mass* | | | | |
| $PM_{2.5}$ (μg m$^{-3}$) | 2.78 ±2.00 | 3.42 ±1.06 | 1.65 ±1.90 | 2.74 ±1.78 |
| $PM_{coarse}$ (μg m$^{-3}$) | 9.35 ±4.74 | 12.24 ±1.89 | 7.49 ±5.17 | 6.62 ±4.09 |
| $PM_{10}$ (μg m$^{-3}$) | 12.13 ±6.05 | 15.65 ±2.37 | 9.15 ±6.56 | 9.36 ±5.19 |
| *Meteorology* | | | | |
| Temp (°C) | 14.0 ±1.3 | 14.5 ±0.2 | 13.5 ±1.2 | 14.85 ±1.4 |
| RH (%) | 80.4 ±8.4 | 89.9 ±0.9 | 78.1 ±7.6 | 84.17 ±7.9 |
| RR (mm Hr$^{-1}$) | -0.04 ±2.68 | 0.01 ±0.07 | -0.21 ±4.64 | -0.12 ±3.69 |
| Wind Speed (m s$^{-1}$) | 6.74 ±3.08 | 7.92 ±1.31 | 4.18 ±2.03 | 4.91 ±2.46 |
| Wind Direction (°) | 225.3 ±56.2 | 200.5 ±7.7 | 238.8 ±37.9 | 188.85 ±58.6 |

* no standard deviation (n=1); $n_{INPs}$ = 0.0077 L$^{-1}$ with a 95% confidence interval of 0.0041 to 0.0137 L$^{-1}$
** no standard deviation (n=1); $n_{INPs}$ = 0.0006 L$^{-1}$ with a 95% confidence interval of 0.0003 to 0.0014 L$^{-1}$
*** no standard deviation (n=1); $n_{INPs}$ = 0.0053 L$^{-1}$ with a 95% confidence interval of 0.0033 to 0.0077 L$^{-1}$
**** no standard deviation (n=1); $n_{INPs}$ = 0.0006 L$^{-1}$ with a 95% confidence interval of 0.0002 to 0.0021 L$^{-1}$

Particulate matter concentrations were elevated during M1 compared to M2, with $PM_{2.5}$ and $PM_{10}$ mass concentrations of 3.42 (±1.06) μg m$^{-3}$ and 15.65 (±2.37) μg m$^{-3}$, respectively, during M1, and 2.78 (±2.00) μg m$^{-3}$ and 12.13 (±6.05) μg m$^{-3}$, respectively, during M2. Additionally, negative values of $PM_{2.5}$ as derived from TEOM data were observed during M2, which were possibly due to very low mass concentrations with possible losses of particle water or semi-volatile species, as reported by Charron et al. (2004). Notably, local wind speeds were lower during M2 (4.18 ± 2.03 m s$^{-1}$) compared to M1 (7.92 ± 1.31 m s$^{-1}$) suggesting lower SSA generation during M2 compared to M1 (Ovadnevaite et al., 2012). Reanalysis wind data (ERA5) indicate that higher wind speeds were present over the North Atlantic in regions of M2 air mass origin compared to that of M1 (Figure S8 and Figure S9), however the region of maximum wind speeds during M2 was located further from the observation site compared to M1. That is, maximum primary SSA production likely occurred closer to the observation site during M1 compared to M2. Observed changes in $n_{INPs}$ during M1 and M2 are discussed in Section 4.2.

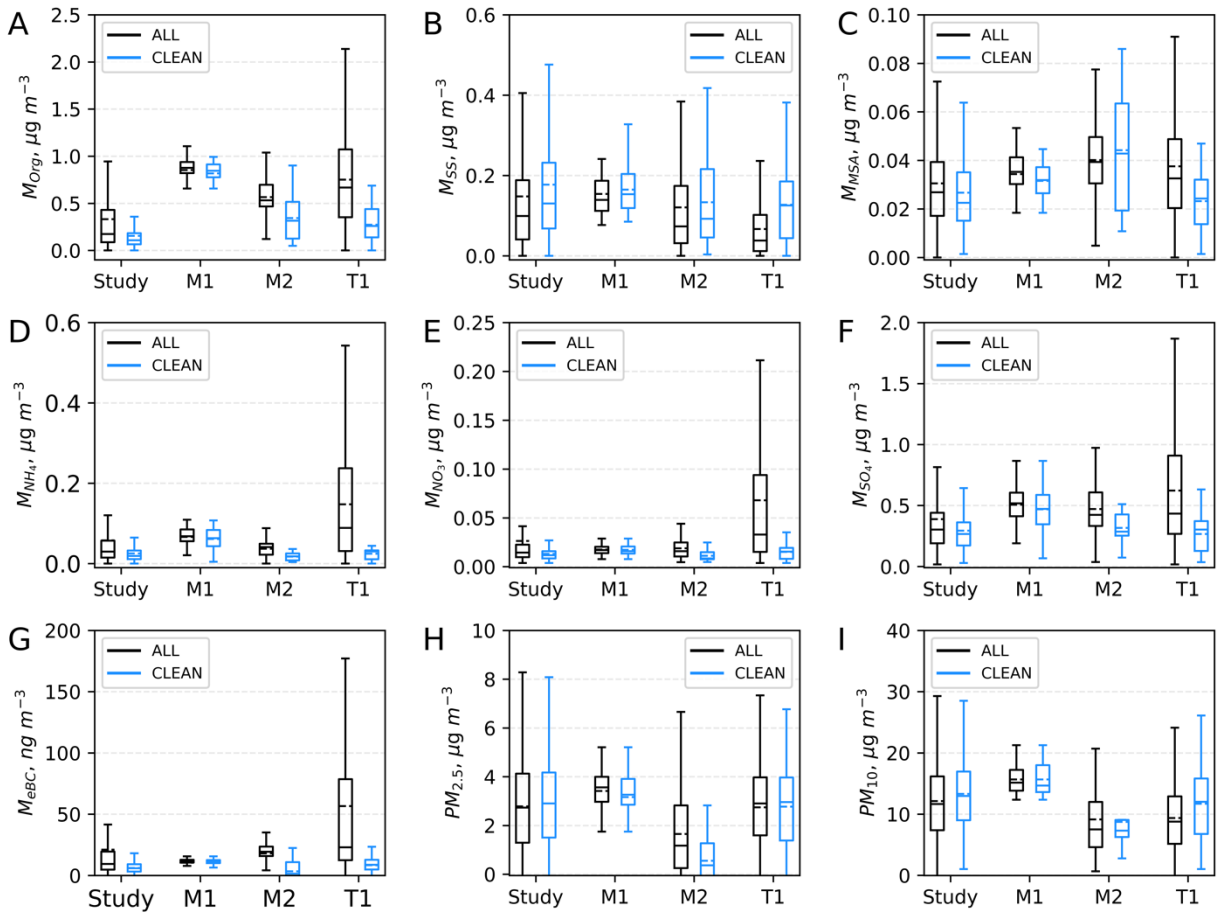


**Figure 2**. Box and whisker plots for ALL (black) and CLEAN (blue) samples for the entire study, marine organic event 1 (M1), marine organic event 2 (M2) and the event with mixed marine and terrestrial air masses (T1). Submicron aerosol ($D_{50}$ < 1 µm) composition data from the HR-ToF-AMS include A) organic matter (Org), B) sea salt (SS), C) methanesulfonic acid (MSA), D), ammonium ($NH_4$), E) nitrate ($NO_3$), and F) sulfate ($SO_4$). Also shown are mass concentrations of G) equivalent black carbon (eBC), H) $PM_{2.5}$ ($D_{50}$ < 2.5 µm), and I) $PM_{10}$ ($D_{50}$ < 10 µm).

Finally, a terrestrial organic event (T1) was sampled by the IS from 15 Aug 11:14 to 20 Aug 11:36. In Figure 3, HYSPLIT back trajectories illustrate that aerosol sampled during this event originated from ocean regions, but passed over southwest Ireland before arriving at MHD (zoomed in map shown in Figure S7). Average $M_{Org}$ were elevated during T1 (0.75 ± 0.53 µg $m^{-3}$) and HR-ToF-AMS mass spectra collected for organic submicron aerosol during T1 (Figure S6) were representative of marine organic aerosol (MSA, m/z 79) mixed with contributions from refined (anthropogenic) hydrocarbons ($C_nH_{2n+1}$, m/z 43, 57 and 71). During T1, mass concentrations of submicron *$NH_4$*, *$NO_3$*, and *eBC* were considerably higher than the study averages (Table 1 and Figure 2), indicating significant influence from land sources. T1 is considered a marine air mass with significant mixing with land-derived aerosol.

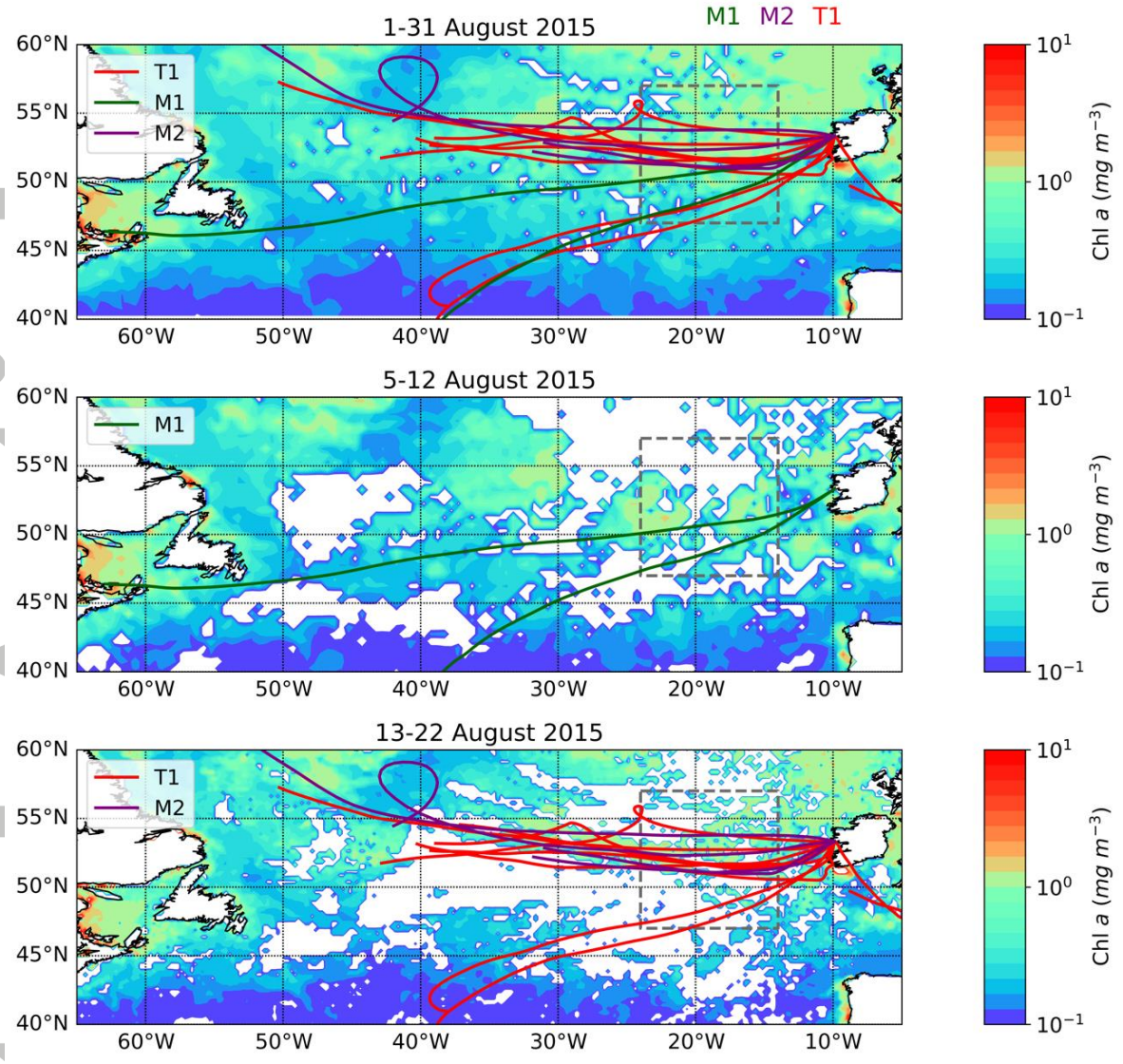


**Figure 3**. Ocean surface Chl *a* concentrations, retrieved from satellite during 1-31 August 2015 (top), 5-12 August 2015 (middle) and 13-22 August 2015 (bottom). Green traces depict HYSPLIT back trajectories during the M1 event; purple traces depict HYSPLIT back trajectories during the M2 event; red traces depict HYSPLIT back trajectory during the T1 event. Grey dashed boxes outline the region used for lag correlation analysis. White regions indicate land regions or areas absent of data. Zoomed in maps over Ireland are shown in Figure S7.

### 4.2 Overview of INP population influences at MHD

Average $n_{INPs,-15\ °C}$ measured by the IS from total suspended aerosol samples were 0.003 (± 0.0033) $L^{-1}$ of air for samples collected continuously (ALL), whereas average CLEAN sector $n_{INPs,-15\ °C}$ were 0.0011 (± 0.0014) $L^{-1}$ of air. Figure 4 includes $n_{INPs}$ as a function of temperature (INP temperature spectrum) for the ALL (Figure 4a) and CLEAN-sector (Figure 4b) samples analyzed by the IS during this study. INP temperature spectra for ALL and CLEAN sector filter pairs collected during the study are provided, in Figure S10. Measured $n_{INPs}$ at MHD are within the range of previous laboratory and field measurements of SSA, with many data falling at the lower range of temperature spectra identified as marine by DeMott et al. (2016).

Figure 4 also includes $n_{INPs}$ measured by the HINC-EV (ALL) and DFPC (CLEAN sector only). HINC-EV measurements of $n_{INPs, -30\ °C}$ fall within an order of magnitude of $n_{INPs}$ estimated from an extrapolation of the IS INP spectra to colder temperatures (Figure 4a), indicating good method agreement based on recent comparisons between ice nucleation measurement techniques (DeMott et al., 2017). At -22 °C in the CLEAN sector, the DFPC measurements of $n_{INPs, -22\ °C}$ from $PM_{10}$ aerosol collections are within an order of magnitude of $n_{INPs, -22\ °C}$ measured by the IS (Figure 4b). DFPC analyses were also performed on $PM_1$ aerosol collections and were often within an order of magnitude of IS and $PM_{10}$ DFPC measurements of $n_{INPs, -22\ °C}$. Agreement between $n_{INPs, -22\ °C}$ measured in $PM_1$ and $PM_{10}$ suggests that the mode sizes of the INP populations measured during this study were often 1 μm or smaller. However, during the terrestrial organic event (T1), $n_{INPs, -22\ °C}$, measured by the DFPC on $PM_1$ aerosol collections, were more than an order of magnitude lower than $n_{INPs, -22\ °C}$ reported from the IS and $PM_{10}$ DFPC measurements, suggesting that a significant proportion of the INP population was larger than 1 μm during T1.

Samples collected over the entire study regardless of wind direction (Figure 4a) illustrate that $n_{INPs}$ varied by a factor of 5-200 when measured at any given temperature warmer than -30 °C, with progressively more variability at warmer temperatures (T > -20 °C). Variability was reduced when measurements were isolated to the CLEAN-sector (Figure 4b), particularly at warmer temperatures, but $n_{INPs}$ were still scattered by over an order of magnitude. These findings remain true after accounting for variations in aerosol surface area (Figure S11). This variability is within the range of previously reported $n_{INPs}$ (DeMott et al., 2016) and indicates that there are complexities in the ice nucleation ability of aerosol that extend beyond the available surface area.

Highlighted in Figure 4c and Figure 4d are the organic events described in Section 4.1 (M1, M2, and T1) for the ALL and CLEAN sector samples, respectively. For the purpose of this discussion, measurements by the HINC-EV and DFPC for these events were confined to those made within the IS filter sampling periods. The presence of terrestrial INPs is evident during T1, where higher $n_{INPs}$ across temperatures warmer than approximately -22 °C (Figure 4c) were observed in the ALL samples analyzed by the IS. No clear enhancement in $n_{INPs}$ was observed in CLEAN sector samples (both IS and DFPC) collected during T1, suggesting the INP population was from a terrestrial source (Figure 4d). No significant enhancement was observed for average $n_{INPs}$ observed by the HINC at -30 °C during T1 compare to the rest of the study.

During the first marine event, M1, $n_{INPs}$ measured in the ALL and CLEAN-sector samples indicate elevated $n_{INPs}$ at temperatures warmer than approximately -22 °C, but little change in $n_{INPs}$ at colder nucleation temperatures. However, HINC measurements of $n_{INPs}$ at -30 °C indicate higher average $n_{INPs}$ during M1 ($3.98 \pm 1.19\ L^{-1}$) compared to the study average ($2.33 \pm 0.87\ L^{-1}$, $p < 0.01$) (Figure 4c). As mentioned previously, *eBC* was slightly above the CLEAN sector threshold during M2 and thus a CLEAN sector sample was not collected during M2 for the IS. Despite this, the concentrations of $n_{INPs}$ observed by the IS during M2 fell within the same range of temperature spectra observed in the CLEAN sector throughout the study and no enhancement in $n_{INPs}$ was observed (Figure 4c). Mass spectra derived by HR-ToF-AMS contained greater contributions of MSA during M2 compared to M1 and lower particulate mass ($PM_{2.5}$), including negative values, as derived from TEOM data. Local wind speed measurements and reanalysis wind speeds suggest that primary SSA production that occurred closer to the measurement site was likely a larger contributor to aerosol during M1 compared to M2. Primary SSA production (i.e., higher wind speeds) during M2 likely occurred further from the observation site (see Figures S5 and S6).

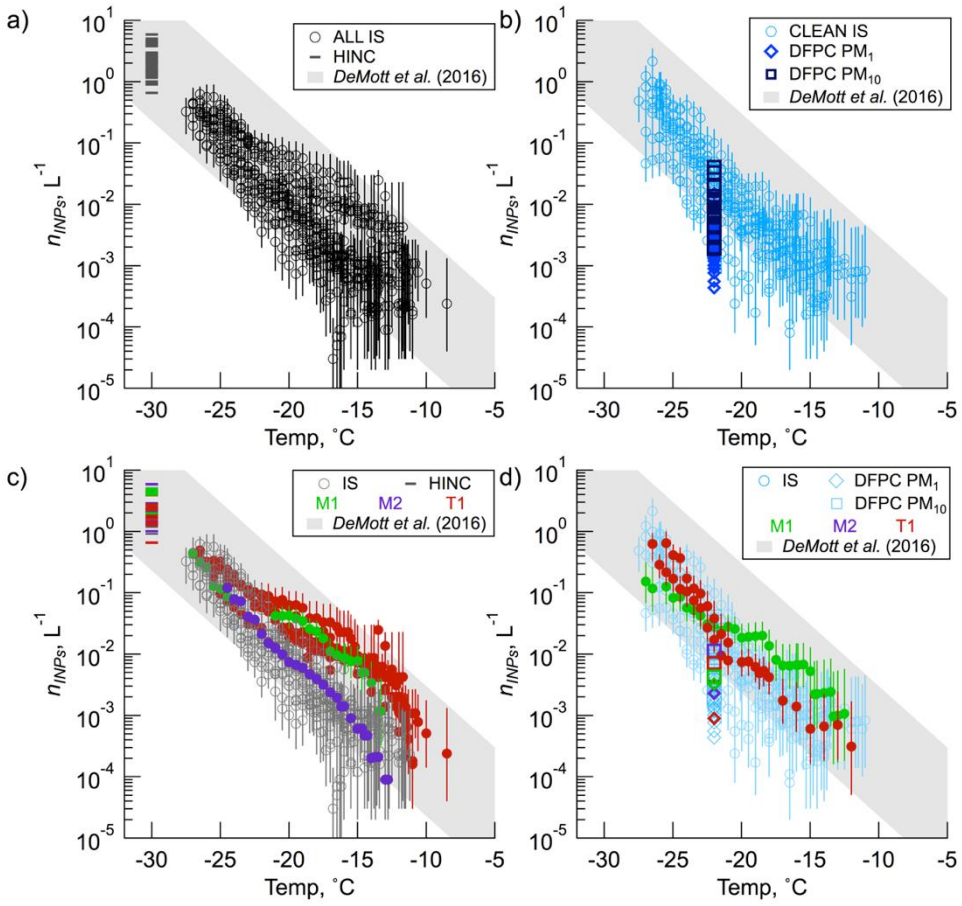


**Figure 4**. INP temperature spectra for a) ALL samples; b) CLEAN sector samples; c) ALL samples with highlighted events; and d) CLEAN sector samples with highlighted events. Data include those from IS (circles), HINC-EV(dash markers) and DFPC $PM_1$ (diamond markers) and $PM_{10}$ (squares). In c), grey open circles correspond to ALL aerosol for a given collection period. In d), light blue open circles correspond to aerosol collected in the CLEAN sector only. In c) and d), green, purple and red filled circles correspond to the INP concentrations measured by the IS during the M1, M2 and T1 organic events, respectively. HINC-EV and DFPC are also highlighted for each organic event. The light grey shaded area represents the range of values reported by DeMott et al. (2016) for nascent laboratory-generated and ambient SSA.

Studies have reported lower enrichments of organic matter in submicron SSA associated with higher wind speeds (Gantt et al., 2011; Rinaldi et al., 2013) and have suggested that higher wind speeds lead to increased mixing of the surface organic layer with sub-surface water, reducing the organic enrichment in the SML, thereby reducing in the amount of organic matter transferred to the submicron aerosol. Other processes, including chemical selectivity (Cochran et al., 2016; van Pinxteren et al., 2017) and film versus jet drop formation (Wang et al., 2017), have also been shown as important parameters that control the specific compounds or particulates that comprise the organic fraction of SSA, which will ultimately control the number of INPs. For example, Rinaldi et al. (2013) developed a source function for predicting submicron sea spray organic matter based on Chl *a* and wind speed and assuming marine organic matter was comprised of water insoluble organic matter. van Pinxteren et al. (2017) showed that this source function for submicron sea spray organic matter (Rinaldi et al., 2013) under-predicted moderately high mass concentrations of sea spray organic matter. van Pinxteren et al. (2017) suggest that non-Chl *a* descriptors of

biological productivity (e.g., bacteria abundance) or other meteorological parameters (e.g., sea surface temperature) may be important variables that can also change the makeup of organic marine aerosols. These parameters also have direct implications for the release of INPs from the ocean surface. Marine INPs have been identified as both ice nucleation active molecules and microbial constituents, depending on bloom conditions (McCluskey et al., 2018). Furthermore, studies have observed enhanced concentrations of INPs in SML samples compared to the underlying bulk seawater (Wilson et al., 2015), while other studies have observed no difference in INP concentrations in the SML and bulk seawater. While all the factors that lead to an increase in $n_{INPs}$ during M1 but not in M2 are not known, it is possible that primary SSA production was a larger contributor to the aerosol measured during M1 than during M2. M2 was associated with lower local wind speeds, maximum primary SSA production further from observation site, greater contribution of MSA to the submicron mass, and lower $PM_{2.5}$. We note that wind speeds increased towards the end of the M2 period (Figure 1) and corresponding elevated $n_{INPs}$ were not observed, suggesting that wind speed alone is a not a sufficient predictor of $n_{INP.}$ Regardless, these data suggest that the INP populations observed during M1 was augmented by additional INPs active at temperatures warmer than -22 °C that were not present during M2 or other CLEAN measurements.

### 4.3 Heat sensitivity and inferred compositions of INPs

INP population types were separated based on INP temperature spectral shapes and comparisons between ALL and CLEAN sector sample pairs. The first spectral shape was log-linearly increasing $n_{INPs}$ with decreasing temperature in both ALL and CLEAN sector sample pairs. The second spectral shape also included log-linear increases in $n_{INPs}$ with decreasing temperature and was augmented by higher $n_{INPs}$ at temperatures warmer than -22 °C. The second spectral type was also the same for ALL and CLEAN sector sample pairs. Finally, spectral shapes that were different from their CLEAN sector pair, or did not have a CLEAN sector pair, comprised the third spectral type. INP population types were classifications were informed by submicron aerosol composition, offline treatments, and air mass back trajectories (Figure 3).

The most commonly observed INP temperature spectral type (19 out of 25 sample pairs) was identified by $n_{INPs}$ increasing approximately log-linearly with decreasing temperature for both CLEAN and ALL samples (Figure 5a). This INP type likely represents a regional INP population that may be representative of a variety of sources, but the source apportionment is not attempted here. However, we note that this INP type was found in both CLEAN sector and ALL samples, suggesting that a major regional source of INPs was from the CLEAN sector. In order to determine heat sensitivity and organic makeup of this INP population type, offline heating and $H_2O_2$ digestion treatments were performed on the filter pair collected from 10 August 18:16 to 11 August 13:37. For the filter set used to represent this first INP type, the BC and wind conditions during the entire sampling duration met CLEAN sector conditions and thus the CLEAN and ALL filter samples contained the same aerosol and corresponding INP population (i.e., replicate samples). This was further supported by the agreement between the ALL and CLEAN INP temperature spectra, shown in Figure 5d. Heating of this sample subset revealed that this population was heat-stable, with no statistically significant difference (i.e., $p > 0.05$, see methods) observed between untreated and heated samples (Figure 5d). However, hydrogen peroxide digestion treatment on this INP type sample subset resulted in a significant reduction in INPs across all temperatures (Figure 5d), indicating that organic matter was a major component of the particles that serve as INPs. This INP type is classified as a Marine Organic INPs, supported by the CLEAN sector origin and the large contribution of organic INPs.

Figure 5b presents the second INP temperature spectral type, where the INP population is augmented by additional INPs active at temperatures warmer than -22 °C in both CLEAN and ALL samples (Section 4.2). This INP type comprises the INP population observed during M1 (9 August from 11:43 to 19:10). Similar to the Marine Organic INP population, the ALL and CLEAN sector INP spectra were not statistically different and CLEAN sector conditions were met for 87% of the sample duration (7.5 hours). Heat treatment was applied to the ALL sample to determine the heat sensitivity of this INP type. This INP population was heat labile (Figure 5e), suggesting that most ice nucleation active material contained proteins or other biological material that was deformed or disaggregated by 95 °C heat. Hydrogen peroxide treatments were not performed on M1 samples due to limited sample availability, so the total contribution of organic matter to these INPs is unknown. Based on the results of these treatments, this INP population was classified as Marine Organic Augmented INPs, and was present for approximately 0.5 days at MHD.

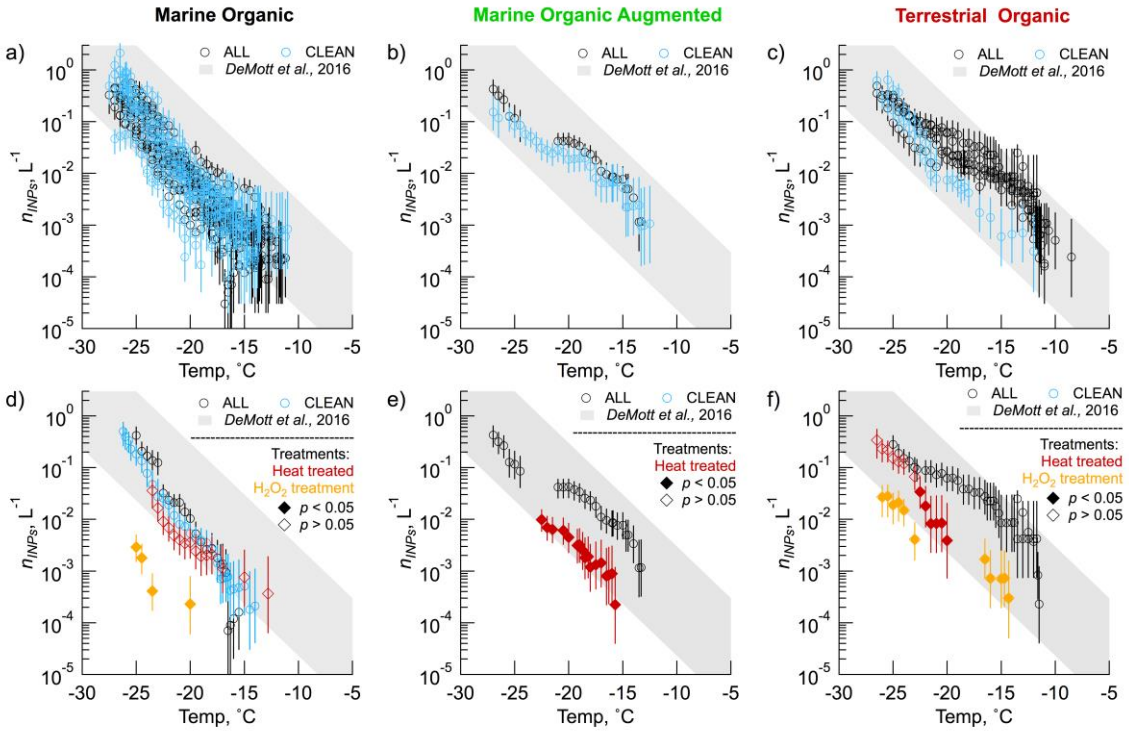


**Figure 5**. Panels a-c) show the three main INP spectral types observed at MHD: (a,d) Marine Organic, (b,e) Marine Organic Augmented and (c, f) Terrestrial Organic. INP spectral resulting from offline treatments performed on samples that are representative of the three classes of INP populations are shown as diamonds in d-f. d) 26-24 Aug, 2015 represents the Marine Organic INP spectral type; e) 9 Aug, 2015 represents the Marine Organic Augmented INP spectral type; and f) 17-18 Aug, 2015 represents the Terrestrial Organic INP spectral type. Blue and black markers correspond to CLEAN sector and ALL samples. Red markers correspond to the heat-treated samples and gold markers correspond to hydrogen peroxide digested samples. Filled diamonds indicate values in treated samples that are statistically significantly different ($p$ <0.05) from untreated samples. Vertical bars are the 95% confidence intervals for IS measurements.

The final INP spectral type was identified by INP temperature spectra that had elevated $n_{INPs}$ across all temperatures warmer than approximately -22 °C in the ALL sample compared to the CLEAN sector samples. This INP population type included all samples from T1. Distinct from the marine INP populations, this elevated $n_{INPs}$ feature was not observed in

the CLEAN-sector (Figure 5c). This INP population was observed on 5 out of 25 total study samples (total event duration of 6 days). HYSPLIT back trajectory analyses and the presence of elevated terrestrial chemical markers (*$NH_4$*, *$NO_3$* and *eBC*) indicate that the land was a contributor to the aerosol during these sampling times. Offline treatments were performed on samples collected from 10:35 17 August to 10:35 18 August and revealed that this INP type was also heat labile and largely comprised of organic matter (Figure 5f). The remaining INPs detected in the $H_2O_2$ treated sample suspensions from T1 is consistent with a higher base level of refractory and likely soil mineral particles. The terrestrial origin and offline treatment results suggest that the INPs are from organic-rich soils, which have been reported as a potentially important source of INPs to the atmosphere (O'Sullivan et al., 2014; Tobo et al., 2014). Based on these results, this INP population type was classified as terrestrial organic aerosol INPs.

### 4.4 Relating marine organic INPs to offshore biological activity

Previous studies have examined the relationship between marine organic aerosol and offshore biological activity at MHD (e.g., O'Dowd et al., 2004, Rinaldi et al., 2013, O'Dowd et al., 2015). Rinaldi et al. (2013) found that increases in submicron organic aerosol arising from biological productivity lags Chl *a* concentrations by 8 days. A similar but somewhat shorter lag between $n_{INPs}$ and Chl *a* is supported based on laboratory studies of nascent SSA (McCluskey et al., 2017), where increases in $n_{INPs}$ occurred 3-4 days after peak Chl *a* concentrations. Here, we use offshore Chl a concentrations, observed from satellite (sample box of 47 to 57 °N and 14 to 24 °W, shown in Figure 3) to determine the utility of Chl *a* as a predictor for marine organic $n_{INPs}$ in ambient aerosol. The relationship between Chl *a* and $n_{INPs}$ (measured by the IS and DFPC for samples of air masses arriving from the CLEAN sector) was tested for lag-correlation coefficients calculated for 0 – 14 day lags.

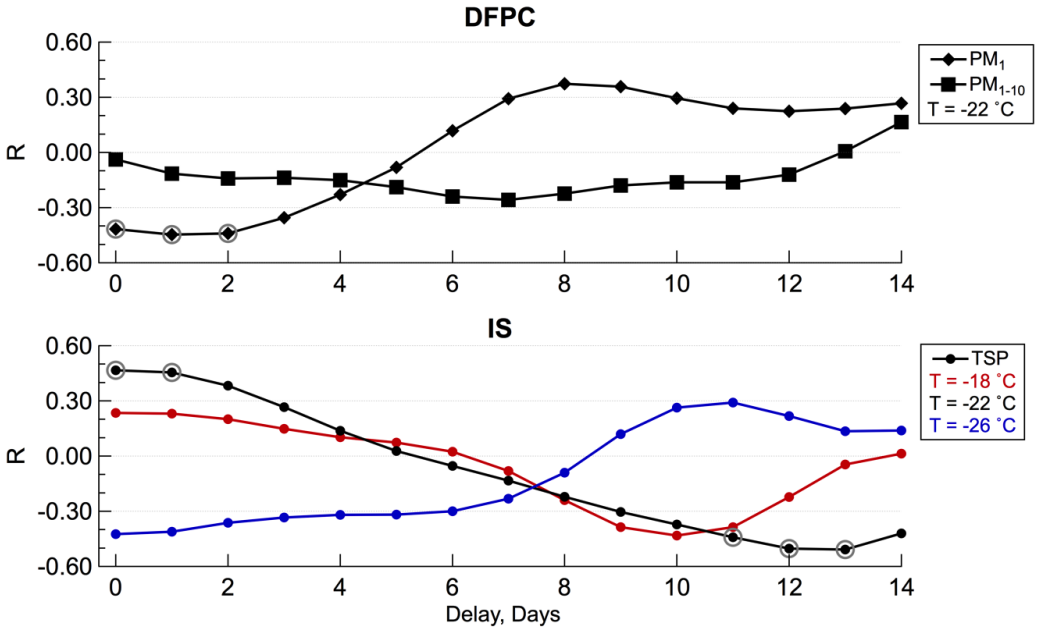


**Figure 6**. Correlation coefficients between Chl *a* and $n_{INPs}$ as a function of the delay time, for (top) $PM_1$ and $PM_{1\text{-}10}$, measured by the Dynamic Filter Processing Chamber (T =-22 °C and $S_w$ >1), and (bottom) total suspended particles, measured by the Ice Spectrometer (T = -18, -22, and -26 °C). Grey circles indicate correlation coefficients significant at the 95% confidence level.

Correlations between Chl *a* and INPs measured by the DFPC at -22 °C were calculated, shown in Figure 6, for both $PM_1$ and $PM_{1\text{-}10}$ ($1 < D_p < 10$ μm), revealing that $n_{INPs}$ were not statistically significantly positively correlated with Chl *a* concentrations. Lag-correlation results for INPs measured by the IS (total suspended particles, or TSP) at -18, -22 and -26 °C are also shown in Figure 6. $n_{INPs}$ were statistically significantly anti-correlated after 11-13 days and at 0-2 days for INPs active at -22 °C in $PM_1$ measured by the DFPC. While a physical reasoning for an anti-correlative relationship between INPs and Chl a is not elaborated on here, these results suggest that, unlike primary marine organic aerosol (e.g., Rinaldi et al., 2013), if increases in ocean biological productivity leads to increased INP emissions, the link is not described by a lag-correlation between $n_{INPs}$ and ocean phytoplankton biomass concentration (i.e., Chl *a*). It is worth highlighting that, different from Rinaldi et al. (2013), the above correlation analysis was performed on a small number of samples, covering only a short time span, characterized by limited Chl-a concentration variability.

These analyses also illustrate that the relationship between $n_{INPs}$ and Chl *a* in nature is likely different across different ice nucleation temperatures and may be sensitive to particle size. The lack of a clear relationship between $n_{INPs}$ and Chl *a* found in this study is consistent with previous measurements of nascent SSA by McCluskey et al. (2017). In that study, INP temperature spectra collected over the course of phytoplankton blooms revealed that increases in $n_{INPs}$ occurred only for INPs in specific temperature ranges, during peak INP emission periods. While determining the size of marine INPs remains an active area of research, many studies have illustrated that the organic enrichment in SSA from ocean biological activity is strongly dependent on particle size (e.g., O'Dowd et al., 2004, Gantt et al., 2013). Future studies should aim to characterize size-dependent $n_{INPs}$ across all temperatures (e.g., Mason et al., 2015) during multiple marine organic events to investigate the relationship between Chl *a* and $n_{INPs}$ across a range of temperatures of activity, Chl *a*, and marine organic aerosol concentrations.

### 4.5 Relating marine organic INPs to organic aerosol mass concentrations

Motivated by evidence suggesting that marine INPs originate from organic matter present in the sea surface microlayer (SML), Wilson et al. (2015) developed an empirical relationship describing the cumulative number of INPs per gram of total organic carbon (TOC, expressed as g of C) in SML samples collected from the North Atlantic and Arctic Oceans, as a function of temperature. To estimate the number of INPs potentially present in SSA, Wilson et al. (2015) applied this empirical relationship to modeled primary marine organic aerosol by assuming the ice nucleation properties of the TOC in simulated emitted SSA particles were equal to that of the organic matter in their SML samples. At the time, concurrent ambient measurements of marine aerosol composition and $n_{INPs}$ were not available to provide more insight into the relationship between TOC and INPs in ambient marine aerosol. The CLEAN sector observations made at MHD as part of this study provide the first opportunity to test how well this assumption agrees with ambient atmospheric aerosols and INPs, following this expression:

$$n_{INP} = (\exp(11.2186 - (0.4459 \times T))) \times TOC$$

where $n_{INPs}$ is the ambient number concentration ($m^{-3}$) of INPs active at a given temperature ($T$, °C) and $TOC$ (g of C per $m^{-3}$ of air) is the total organic carbon mass concentration measured in the ambient aerosol. In order to match the definition of the TOC used by Wilson et al. (2015) to develop this relationship, some approximations were made to estimate aerosol phase TOC for the MHD observations. We estimate $TOC$, termed here as $TOC_{est}$, from the

submicron organic aerosol mass concentration measured by the HR-ToF-AMS ($M_{Org,\ HR\text{-}ToF\text{-}AMS}$) as follows:

$$TOM_{est} = M_{Org,HR-ToF-AMS} \times \frac{POM_{tot}}{POM_{sub}}$$

$$TOC_{est} = \frac{TOM_{est}}{OM:OC}$$

Supermicron aerosol significantly contributes to the total mass of sea spray organic matter (e.g., Facchini et al., 2008). To account for this, a factor of 2 is assumed for the ratio of total particulate organic matter to submicron particulate organic matter ($POM_{tot}/POM_{sub}$), following the best estimate reported by Burrows et al. (2013). A range of $POM_{tot}/POM_{sub}$ (1.4 to 2.5, Burrows et al., 2013) is also tested and used as lower and upper limits of predicted $n_{INPs}$. The OM:OC ratio of sea spray organic matter is assumed to be 2.0, determined based on measured OM:OC of 2.0 and 1.99 for M1 and M2 respectively, by the HR-ToF-AMS.

Results from this exercise are shown in Figure 7, where we compare the predicted $n_{INPs}$ to observed $n_{INPs}$ for INPs active at -15 and -20 °C in CLEAN sector samples. These estimates indicate that the Wilson et al. (2015) relationship over predicts $n_{INPs}$ measured in the CLEAN sector (i.e., pristine marine aerosol) by a factor of 4 to 100, with one third (9 out of 27) of the periods evaluated agreeing within an order of magnitude. A tendency to overpredict $n_{INPs}$ is consistent with an evaluation of the Wilson et al. (2015) approach using measurements of INPs and total organic carbon in nascent laboratory-generated SSA (McCluskey et al., 2017). Similarily, experiments have found differing composition and organic volume fractions for jet drops versus film drops, indicating that the composition and ice nucleation ability of sea spray organic matter is not equal to the composition and ice nucleation ability of the SML (Wang et al., 2017).

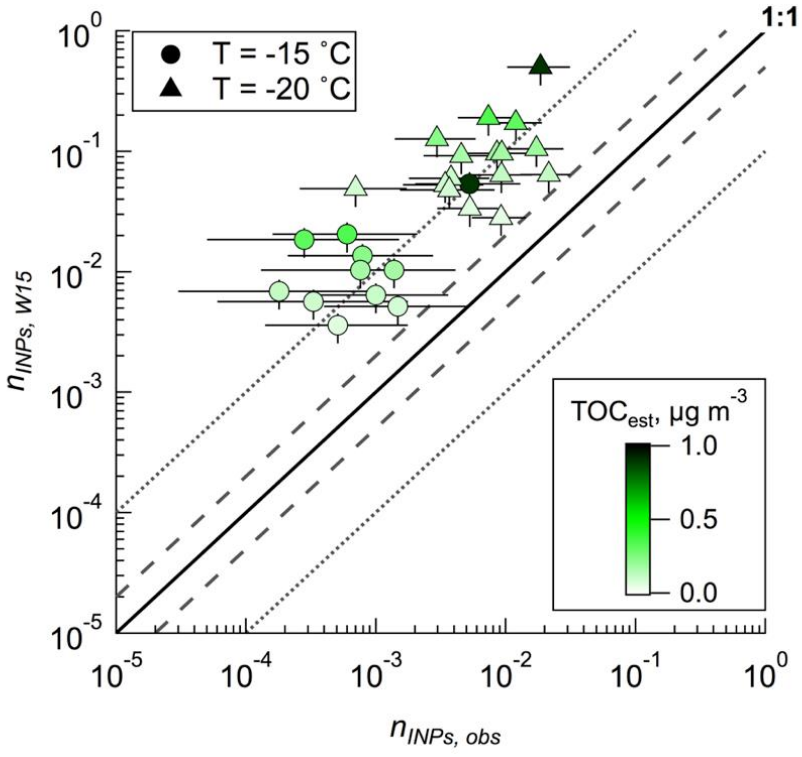


**Figure 7**. Predicted $n_{INPs}$ using Wilson et al., (2015) compared to observed $n_{INPs}$ at -15 °C (circle markers) and -20 °C (triangle markers) in total suspended aerosol from the CLEAN

sector. Points are colored based on the estimated TOC ($TOC_{est}$). Vertical uncertainty bars describe the range in estimated $n_{INPs}$ for the range of $POM_{tot}/POM_{sub}$ reported in the literature. Horizontal bars on data points show uncertainties associated with the measurement (95% confidence interval). Lines indicate 1:1 (solid), a factor of 2 from 1:1 (dashed) and a factor of 10 from 1:1 (dotted).

### 4.6 Predicting sea spray aerosol INPs from aerosol surface area

During M1, $n_{INPs}$ were enhanced and heat labile, suggesting that INPs associated with sea spray organic aerosol during M1 were impacted by ocean biological processes. Lag correlations between $n_{INPs}$ and Chl *a* (Section 4.4) indicate a lack of a clear relationship between Chl *a* concentrations and the emissions of ice nucleation active sea spray organic matter. Discrepancies between observed $n_{INPs}$ and $n_{INPs}$ estimated from the Wilson et al. relationship suggest that additional mechanisms impact the inclusion of INPs from the SML into sea spray organic matter. These exercises clearly demonstrate that much work remains in unraveling the intricacies that lead to episodic periods of elevated $n_{INPs}$ associated with sea spray organic aerosol, such as those observed during M1. However, progress in characterizing ice phase transitions in SSA-cloud interactions requires advancements in scientific understanding and numerical representation of the biological, physical, and chemical mechanisms controlling the emissions and ice nucleation properties of sea spray organic aerosol.

The CLEAN sector measurements at MHD during periods without significant enhancements in $n_{INPs}$ (i.e., excluding M1 measurements) represent pristine SSA and were used to develop a parameterization that describes the typical INP population that is observed in the pristine marine boundary layer in the North Atlantic region. That is, only CLEAN sector Marine Organic INP temperature spectra were used for this parameterization. We follow the approach of Niemand et al. (2012), where the nucleation site density is described as:

$$n_s(T) = \exp(a\,(T - 273.15) + b),$$

where $n_s$ is the nucleation site density ($m^{-2}$), $T$ is temperature (K), and a and b are fit parameters. In this study, $n_s$ was determined based on the IS $n_{INPs}$ and total aerosol surface area, measured by the aerosol size distribution measurements (see Methods), and with the assumption that all particles are representative of one INP type, in this case the Marine Organic INP type. Fit parameters were determined to be -0.545 (± 0.01) and 1.0125 (± 0.29), respectively, for our data. The exponential fit to the CLEAN Marine Organic INP spectra is shown in Figure 8, with a coefficient of determination of 0.821.

This parameterization should be used to specify immersion freezing ice nucleation properties unique to SSA, and could be used to improve estimates of primary ice formation in numerical models that simulate SSA. A comparison between the proposed SSA parameterization and the ice nucleation site density parameterization for mineral dust (Niemand et al., 2012, Figure 8) illustrates that mineral dust is associated with a factor of 1000 more ice nucleating sites per surface area of aerosol compared to SSA. Representing these distinct aerosol sources and their corresponding ice nucleating ability is likely important for modeling INP populations in oceanic regions. The parameterization proposed from this data provides a tool for beginning to explore the impacts of sea spray aerosol on primary and subsequent secondary ice processes in numerical modeling studies. However, we emphasize that this parameterization does not yet incorporate heat labile organic INPs, which were demonstrated as an important component of the INPs observed during the Marine Organic Augmented INP event. Extending this parameterization to include episodic dependencies on

ocean biology and organic matter may be possible with more observations and advanced understanding of the physico-chemical mechanisms that control the composition of sea spray organic matter.

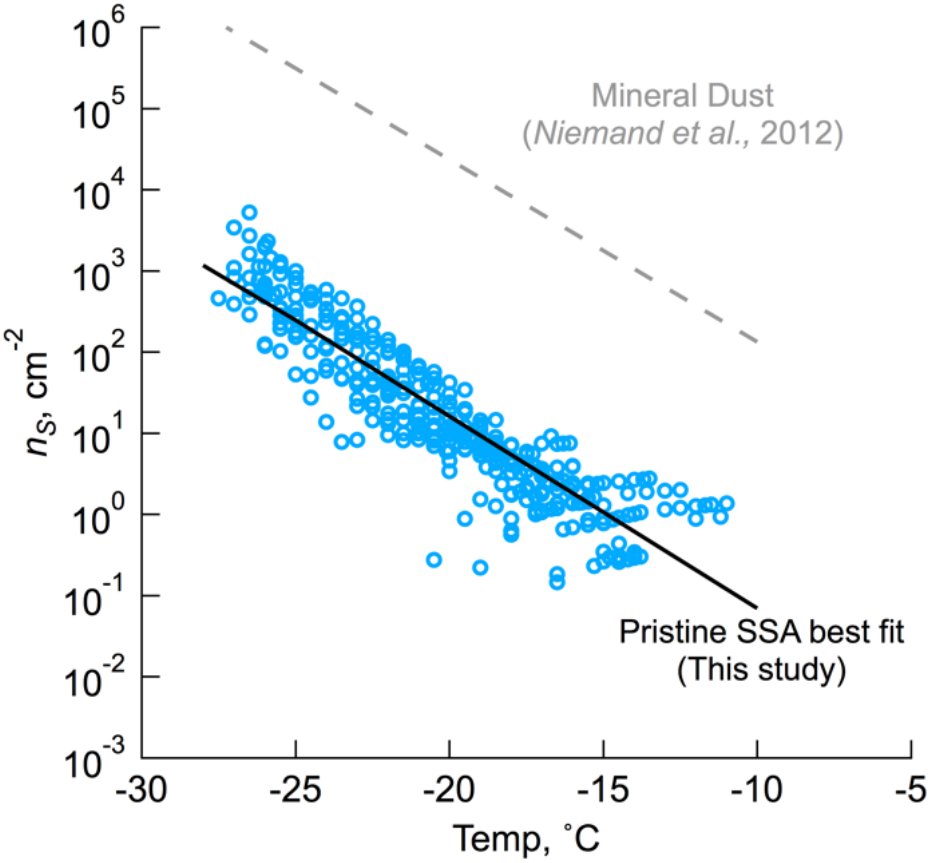


**Figure 8**. Nucleation site densities as a function of temperature measured in the CLEAN sector by the Ice Spectrometer. An exponential fit to the data ($R^2$ = 0.821) is also shown, following the approach by Niemand et al. (2012); the equation for this exponential fit for data is $n_s$ = exp(-0.545($T$-273.15)+1.0125), where $n_s$ is the nucleation site density ($m^{-2}$) and $T$ is temperature (K). Also shown is the parameterization for mineral dust $n_s$ proposed by Niemand et al. (2012).

## 5 Summary

In August 2015, ice nucleation measurement methods were deployed at the Mace Head Research Station (MHD), a remote coastal location at which marine organic aerosol arising from offshore biological activity is commonly observed. Observed INP number concentrations ($n_{INPs}$) at MHD were within previously reported measurements for marine environments, with the largest variability in number concentrations occurring for ice nucleation temperatures warmer than -22 °C. To investigate factors contributing to the variability in $n_{INPs}$, three periods of elevated organic aerosol mass concentrations were examined for changes in meteorology; off-shore biological activity, aerosol organic composition, and properties of INPs (heat sensitivity and organic makeup). The first marine organic event (M1) was associated with higher numbers of $n_{INPs}$ active at temperatures warmer than -22 °C. INPs observed during M1 were heat labile, indicating the presence of protein-containing primary marine organic INPs. A second marine organic event (M2) was

observed during the study, but was associated with no change in observed INPs, potentially due to differences in organic composition that may have been a consequence of lower wind speeds closer to the observation site compared to M1, biological processes that are not described fully by Chl *a* (e.g., bacteria abundances) or other variables that are currently unknown. Finally, marine aerosol that was significantly influenced by terrestrial aerosol (T1) was associated with increased $n_{INPs}$, and the INP population that was present during this period was heat labile and was largely made up of organic material.

Offshore ocean Chl *a* and organic aerosol mass concentrations were explored as possible predictors for the changes in $n_{INPs}$ associated with marine organic aerosol events. Lag correlation analyses show a lack of a clear relationship between $n_{INPs}$ and Chl *a*, and the utility of Chl *a* as a predictor for INP emissions likely requires detailed evaluations on how this relationship changes across different ice nucleation temperatures and particle sizes. Predictions of $n_{INPs}$ based on organic carbon mass concentrations (Wilson et al., 2015) over predicted marine $n_{INPs}$ by a factor of 4-100 in this study. While our current understanding of the many factors that control the abundance of episodic heat labile INPs in sea spray organic aerosol is inadequate to numerically describe their behavior, we propose a parameterization that describes the nucleation site density of the typical marine organic INP population observed in the marine boundary layer at MHD, revealing a factor of 1000 lower ice nucleation site density associated with SSA compared to mineral dust (Niemand et al., 2012).

## Acknowledgments, Samples, and Data

The authors would like to acknowledge Jake Zaragoza for his contributions to the ice spectrometer analyses. The satellite products used in this paper were processed and distributed by ACRI-ST GlobColour service, supported by the EU FP7 MyOcean and ESA GlobColour projects, using ESA Envisat MERIS and NASA MODIS and SeaWiFS data. Reanalysis wind data were sourced from the European Centre for Medium-Range Weather Forecasts. (2017, updated monthly. *ERA5 Reanalysis*. Research Data Archive at the National Center for Atmospheric Research, Computational and Information Systems Laboratory. https://doi.org/10.5065/D6X34W69. Accessed 06 03 2018).The research leading to these results has received funding from the European Union's Seventh Framework Programme (FP7/2007-2013) project BACCHUS under grant agreement no. 603445 and from the National Science Foundation (AGS-1358495). This work was also supported by the CNR (Italy) under Air-Sea Lab: Progetto Laboratori Congiunti. C. S. M. also acknowledges travel support from the Colorado State University Department of Atmospheric Science ASCENT (Assisting Students, Cultivating Excellence, Nurturing Talent) Travel Award. The National Center for Atmospheric Research is sponsored by the National Science Foundation. The data used are listed in the references, tables, supporting information, and in a digital repository at Colorado State University (https://hdl.handle.net/10217/187808).

## References

Allan, J. D., M. R. Alfarra, K. N. Bower, P. I. Williams, M. W. Gallagher, J. L. Jimenez, A. G. McDonald, E. Nemitz, M. R. Canagaratna, J. T. Jayne, H. Coe, and D. R. Worsnop, (2003), Quantitative sampling using an Aerodyne aerosol mass spectrometer: 2. Measurements of fine particulate chemical composition in two UK cities, *J Geophys Res-Atmos*, 108 (4091).

Agresti A., & B. A. Coull, (1998), Approximate is better than “exact” for interval estimation of binomial proportions. *Am. Stat.*, 52, 119–126.

Bigg, E. K. (1973), Ice nucleus concentrations in remote areas, *Journal of Atmospheric Science*, 30, 1153–1157.

Belosi, F., M. Rinaldi, S. Decesari, L. Tarozzi, A. Nicosia, G. Santachiara, (2017), Ground level ice nuclei particle measurements including Saharan dust events at a Po Valley rural site (San Pietro Capofiume, Italy), *Atmospheric Research*, 186, 116-126, doi:10.1016/j.atmosres.2016.11.012.

Burrows, S. M., C. Hoose, U. Pöschl, and M. G. Lawrence, (2013), Ice nuclei in marine air: biogenic particles or dust? *Atmospheric Chemistry and Physics*, 13, 245–267, doi:10.5194/acp-13-245-2013.

Canagaratna, M. R., J. T. Jayne, J. L. Jimenez, J. D. Allan, M. R. Alfarra, Q. Zhang, T. B. Onasch, F. Drewnick, H. Coe, A. Middlebrook, A. Delia, L. R. Williams, A. M. Trimborn, M. J. Northway, P. F. DeCarlo, C. E. Kolb, P. Davidovits, and D. R. Worsnop, (2007), Chemical and microphysical characterization of ambient aerosols with the aerodyne aerosol mass spectrometer, *Mass Spectrom Rev*, 26, 185-222.

Charron, A., R. M. Harrison, S. Moorcroft, J. Booker, (2014), Quantitative interpretation of divergence between PM and PM mass measurement by TEOM and gravimetric (Partisol) instruments, *Atmospheric Environment*, 38, 3, 415-423, doi:10.1016/j.atmosenv.2003.09.072.

Cochran, R. E., and Coauthors, (2016), Analysis of Organic Anionic Surfactants in Fine and Coarse Fractions of Freshly Emitted Sea Spray Aerosol. *Environmental Science Technology*, 50, 2477–2486, doi:10.1021/acs.est.5b04053.

DeCarlo, P. F., Kimmel, J. R., Trimborn, A., Northway, M. J., Jayne, J. T., Aiken, A. C., Gonin, M., Fuhrer, K., Horvath, T., Docherty, K. S., Worsnop, D. R., and Jimenez, J. L., (2006), Field-deployable, high-resolution, time-of-flight aerosol mass spectrometer, *Analytical Chemistry*, 78, 8281-8289, doi:10.1021/Ac061249n.

DeMott, P. J., and Coauthors, (2016), Sea spray aerosol as a unique source of ice nucleating particles. *Proceedings of the National Academy of Science U.S.A.*, 113, 5797–5803.

DeMott, P. J., and Coauthors, (2017), Comparative measurements of ambient atmospheric concentrations of ice nucleation particles using multiple immersion freezing methods and a continuous flow diffusion chamber, *Atmos. Chem. Phys*., 17, 11227-11245, doi: 10.5194/acp-17-11227-2017.

Facchini, M. C., and Coauthors, (2008), Primary submicron marine aerosol dominated by insoluble organic colloids and aggregates, *Geophysical Resesarch Letters*, 35, L17814, doi:10.1029/2008GL034210.

Gantt, B., Meskhidze, N., Facchini, M. C., Rinaldi, M., Ceburnis, D., and O'Dowd, C. D., (2011), Wind speed dependent size-resolved parameterization for the organic mass fraction of sea spray aerosol, *Atmospheric Chemistry and Physics*, 11, 8777-8790, https://doi.org/10.5194/acp-11-8777-2011.

Gantt, B., and N. Meskhidze, (2013), The physical and chemical characteristics of marine primary organic aerosol: a review, *Atmospheric Chemistry and Physics*, 13, 3979–3996, doi:10.5194/acp-13-3979-2013.

Ghil, M., M. R. Allen, M. D. Dettinger, K. Ide, D. Kondrashov, M. E. Mann, A. W. Robertson, A. Saunders, Y. Tian, F. Varadi, and P. Yiou, (2002), Advanced spectral methods for climatic time series, *Reviews of Geophysics*, 40(1), 1003, doi:doi:10.1029/2000RG000092.

Govindarajan, A. G. and Lindow, S. E., (1988), Size of bacterial ice-nucleation sites measured in situ by radiation inactivation analysis. *Proceedings of the National Academy of Science U.S.A.*, 85, 1334-1338.

Hill, T. C. J., P. J. DeMott, Y. Tobo, J. Fröhlich-Nowoisky, B. F. Moffett, G. D. Franc and S. M. Kreidenweis, (2016), Sources of organic ice nucleating particles in soils. *Atmos. Chem. Phys.*, 16, 7195–721.

Huang, Y., A. Protat, S. T. Siems, and M. J. Manton, (2015), A-Train Observations of Maritime Midlatitude Storm-Track Cloud Systems: Comparing the Southern Ocean against the North Atlantic. *Journal of Climate*, 28, 1920–1939, doi:10.1175/JCLI-D-14-00169.1.

Jimenez, J. L., Jayne, J. T., Shi, Q., Kolb, C. E., Worsnop, D. R., Yourshaw, I., Seinfeld, J. H., Flagan, R. C., Zhang, X. F., Smith, K. A., Morris, J. W., and Davidovits, P., (2003), Ambient aerosol sampling using the Aerodyne Aerosol Mass Spectrometer, *Journal of Geophysical Research Atmospheres*, 108, 8425, doi:10.1029/2001JD001213, 2003.

Kanji, Z. A., and Abbatt, J. P. D., (2009), The University of Toronto Continuous Flow Diffusion Chamber (UT-CFDC): A Simple Design for Ice Nucleation Studies, *Aerosol Science and Technology*, 43, 730-738, 10.1080/02786820902889861.

Kleefeld, C., and Coauthors, (2002), The relative contribution of submicron and supermicron particles to aerosol light scattering in the marine boundary layer (MBL), *Journal Geophysical Research*, 107(D19), 8103, doi:10.1029/2000JD000262.

Lacher, L., and Coauthors, (2017), The Horizontal Ice Nucleation Chamber (HINC): INP measurements at conditions relevant for mixed-phase clouds at the High Altitude Research Station Jungfraujoch *Atmos. Chem. Phys.*, 17, 15199–15224, doi: 10.5194/acp-17-15199-2017

Ladino, L. A., J. D. Yakobi-Hancock, W. P. Kilthau, R. H. Mason, M. Si, J. Li, L. A. Miller, C. L. Schiller, J. A. Huffman, J. Y. Aller, D. A. Knopf, A. K. Bertram, J. P. D. Abbatt, (2016), Addressing the ice nucleating abilities of marine aerosol: A combination of deposition mode laboratory and field measurements, *Atmos. Environ.*, doi: 10.1016/j.atmosenv.2016.02.028.

Langer, G., Rodgers, J., (1975), An experimental study of ice nuclei on membrane filters and other substrata. *Journal of Applied Meteorology*, 14, 560–571.

Mason, R., and Coauthors, (2015), Ice nucleating particles at a coastal marine boundary layer site: correlcations with aerosol type and meteorological conditions. *Atmospheric Chemistry and Physics*, 15, 12547-12566, doi:10.5194/acp-15-12547-2015.

McCluskey, C. S. and Coauthors, (2017), A Dynamic Link between Ice Nucleating Particles Released in Nascent Sea Spray Aerosol and Oceanic Biological Activity during Two Mesocosm Experiments. *Journal of Atmospheric Science*, 74, 151-166, doi:10.1175/JAS-D-16-0087.1

McCluskey, C. S. and Coauthors, (2018) A mesocosm double feature: Insights into the chemical make-up of marine ice nucleating particles. *Journal of Atmospheric Science*, doi: 10.1175/JAS-D-17-0155.1.

McCoy, D. T., D. L. Hartmann, M. D. Zelinka, P. Ceppi, and D. P. Grosvenor, (2015), Mixed-phase cloud physics and Southern Ocean cloud feedback in climate models. *Journal of Geophysical Research Atmospheres*, 120, 9539–9554, doi:10.1002/2015JD023603.

McCoy, D. T., I. Tan, D. L. Hartmann, M. D. Zelinka, and T. Storelvmo, (2016), On the relationships among cloud cover, mixed-phase partitioning, and planetary albedo in GCMs, *Journal of Advances in Modeling Earth Systems*, 8, 650–668, doi:10.1002/2015MS000589.

Middlebrook, A. M., Bahreini, R., Jimenez, J. L., and Canagaratna, M. R., (2012), Evaluation of composition-dependent collection efficiencies for the aerodyne aerosol mass spectrometer using field data, *Aerosol Science and Technology*, 46, 258–271, doi:10.1080/02786826.2011.620041.

Niemand, M., and Coauthors, (2012), A Particle-Surface-Area-Based Parameterization of Immersion Freezing on Desert Dust Particles. *Journal of Atmospheric Science*, 69, 3077–3092, https://doi.org/10.1175/JAS-D-11-0249.1

O'Dowd, C. D., and Coauthors, (2004), Biogenically driven organic contributions to marine aerosol. *Nature*, 431, 676-680, doi: 10.1038/nature02959.

O'Dowd, C. and Coauthors, (2015), Connecting marine productivity to sea-spray via nanoscale biological processes: Phytoplankton Dance or Death Disco?, *Scientific Reports*, **5**, 14883, doi: 10.1038/srep14883, 2015.

O'Sullivan, D., and Coauthors, (2014), Ice nucleation by fertile soil dusts: relative importance of mineral and biogenic components, *Atmospheric Chemistry and Physics*, 14, 1853-1867, https://doi.org/10.5194/acp-14-1853-2014.

Ovadnevaite, J., and Coauthors, (2011), Detecting high contributions of primary organic matter to marine aerosol: A case study, *Geophysical Research Letters*, 38, L02807.

Ovadnevaite, J., and Coauthors, (2012), On the effect of wind speed on submicron sea salt mass concentrations and source fluxes, *Journal of Geophysical Research Atmospheres*, 117, doi:10.1029/2011jd017379.

Ovadnevaite, J., D. Ceburnis, S. Leinert, M. Dall'Osto, M. Canagaratna, S. O'Doherty, H. Berresheim, and C. O'Dowd,(2014) Submicron NE Atlantic marine aerosol chemical composition and abundance: Seasonal trends and air mass categorization, *J Geophys Res-Atmos*, **119**, 11850-11863.

Polen, M., E. Lawlis, and R. C. Sullivan, (2016), The unstable ice nucleation properties of Snomax® bacterial particles, *J. Geophys. Res. Atmos.*, 121, 11,666–11,678, doi:10.1002/2016JD025251.

Rinaldi, M., and Coauthors, (2009), On the representativeness of coastal aerosol studies to open ocean studies: Mace Head–a case study. *Atmospheric Chemistry and Physics*, 9, 9635–9646.

Rinaldi, M., and Coauthors, (2010), Primary and Secondary Organic Marine Aerosol and Oceanic Biological Activity: Recent Results and New Perspectives for Future Studies, *Advances in Meteorology*, doi:10.1155/2010/310682

Rinaldi, M., and Coauthors, (2013), Is chlorophyll-a the best surrogate for organic matter enrichment in submicron primary marine aerosol?, *Journal of Geophysical Research Atmospheres*, 118, 4964–4973, doi:10.1002/jgrd.50417.

Sanchez, K. J., and Coauthors, (2017), Top-down and Bottom-up aerosol-cloud-closure: towards understanding sources of uncertainty in deriving cloud radiative flux, *Atmospheric Chemistry and Physics Discussions*, doi:10.5194/acp-2017-201, 2017

Santachiara G., and Coauthors, (2010), Atmospheric particles acting as ice forming nuclei in different size ranges. *Atmospheric Research*., 96, 266-272.

Schnell, R. C., & G. Vali, (1976), Biogenic ice nuclei: Part I. Terrestrial and marine sources, *Journal of Atmospheric Science*, 33(8), 1554-1564.

Schill, G., and M. A. Tolbert, (2014),Heterogeneous Ice Nucleation on Simulated Sea-Spray Aerosol Using Raman Microscopy, *J. Phys. Chem. C*, 118 (50), 29234-29241, doi: 10.1021/jp505379j

Spurny. K. R., and J. P. Lodge, Jr, (1972), Collection efficiency tables—for membrane filters used in the sampling and analysis of aerosols and hydrosols. *NCAR Technical Note* (National Center for Atmospheric Research, Boulder, CO), NCAR-TN/STR-77, Vol I.

Stein, A.F., Draxler, R.R, Rolph, G.D., Stunder, B.J.B., Cohen, M.D., and Ngan, F., (2015), NOAA's HYSPLIT atmospheric transport and dispersion modeling system, *Bulletin of the American Meteorology Society*, 96, 2059-2077, doi: 10.1175/BAMS-D-14-00110.1.

Tan, I., T. Storelvmo, M. D. Zelinka, (2016), Observational constraints on mixed-phase clouds imply higher climate sensitivity, *Science*, 352 (6282), 224-227, doi: 10.1126/science.aad5300

Tobo, Y., and Coauthors, (2014), Organic matter matters for ice nuclei of agricultural soil origin, *Atmospheric Chemistry and Physics*, 14(16), 8521-8531, doi: 10.5194/acp-14-8521-2014.

Vali, G., (1971), Quantitative evaluation of experimental results on the heterogeneous freezing nucleation of supercooled liquids. *Journal of Atmospheric Science*, 28, 402–409, doi:10.1175/1520-0469(1971)028,0402:QEOERA.2.0.CO;2.

van Pinxteren, M., and Coauthors, (2017), The influence of environmental drivers on the enrichment of organic carbon in the sea surface microlayer and in submicron aerosol particles – measurements from the Atlantic Ocean, *Elementa Science of the Anthropocene*, 5, 35, doi:10.1525/elementa.225

Vergara-Temprado, J., and Coauthors, (2017), Contribution of feldspar and marine organic aerosols to global ice nucleating particle concentrations, *Atmospheric Chemistry and Physics*, 17, 3637-3658, doi.org/10.5194/acp-17-3637-2017

Wang, X., and Coauthros, (2017), The role of jet and film drops in controlling the mixing state of submicron sea spray aerosol particles, *Proceedings of the National Academy of Science U.S.A.*, 114(27), 6978-6983.

Wilson, T. W., and Coauthors, (2015), A marine biogenic source of atmospheric ice-nucleating particles. *Nature*, 525, 234–238, doi:10.1038/nature14986.

Zhang, Z.B., Liu, L.S., Wu, Z.J., Li, J., Ding, H.B., (1998), Physicochemical studies of the sea surface microlayer – I. Thickness of the sea surface microlayer and its experimental determination. *Journal of Colloid and Interface Science*, 204, 294–299.